

IJS-TP-96/6
February 1996

THE CONTROVERSY IN THE $\gamma\gamma \rightarrow \rho\rho$ PROCESS: POTENTIAL SCATTERING OR $qq\bar{q}\bar{q}$ RESONANCE ?

Borut Bajc^a, Saša Prelovšek^a and Mitja Rosina^{a,b}

a) *J. Stefan Institute, Jamova 39, P.O.B. 3000, 1001 Ljubljana, Slovenia*

b) *Faculty of Mathematics and Physics, University of Ljubljana, Jadranska
19, P.O.B .64, 1001 Ljubljana, Slovenia*

ABSTRACT

The $\gamma\gamma \rightarrow \rho^0\rho^0 \rightarrow 4\pi$ reaction shows a broad peak at 1.5 GeV in the $(J^P, J_z) = (2^+, 2)$ channel which has no counterpart in the $\rho^+\rho^-$ channel. This "resonance" is considered as a candidate for a $qq\bar{q}\bar{q}$ state in the "s-channel". We show, however, that it can also be explained by potential scattering of $\rho^0\rho^0$ via the σ - exchange in the "t-channel".

1. Introduction

After many successes of quark models to describe a single meson or baryon, their predictive power in the two-hadron sector remains questionable. A fair description of the nucleon-nucleon interaction [1] was accompanied with the prediction of a rich dibaryon spectrum which has never been observed; it is not yet explained whether the predictions are wrong or the levels just too broad. Therefore it is of great interest to see how different quark

models perform in the two-meson sector, as compared to effective mesonic models.

Much experimental and theoretical interest has concentrated in the $\rho\rho$ system. Firstly, there is a remarkable experimental "puzzle". The $\gamma\gamma \rightarrow \rho\rho$ reaction is characterized by the following features [2, 3]: a large and broad peak near the nominal threshold in the $\rho^0\rho^0$ ($2^+, 2$) channel and a much smaller cross section ("noise") in other $\rho^0\rho^0$ channels as well as in the $\rho^+\rho^-$ channel.

Secondly, the $\rho\rho$ system consists of two unstable (shortlived) hadrons. Therefore, the shape of the "resonance" is unusual and it challenges an appropriate quantum mechanical treatment. Also, such shape might be selective regarding competing models. More experimental data would be very welcome in order to sharpen the details of this shape.

A good model should explain all these features simultaneously. Since so far the quark models [4, 5] covered more features simultaneously than the effective mesonic models [6, 7], the opinion prevails that explicit quark degrees of freedom (a $qq\bar{q}\bar{q}$ molecule) are essential for this process. In the present paper we challenge this view. We show that the considered process can also be explained by potential scattering.

Of course, also in potential scattering, the intermediate system consists of two quarks and antiquarks, each $q\bar{q}$ pair being correlated like in a free ρ meson. This is just one important configuration, which also extends into the asymptotic region. Other intermediate $qq\bar{q}\bar{q}$ configurations (such as those suggested in [4, 5]) may or may not be important. They can easily lead to a resonance peak but this does not prove that they really dominate (that they are at the right energy and strongly coupled to the asymptotic wavefunction) unless no other mechanism exists.

The peak near the nominal threshold and its strong spin dependence are reminiscent of the p-n scattering at low energy. There the S=0 channel has an exceptionally high cross section while in the S=1 channel it is much lower. The reason is that in the S=0 state the potential well contains almost exactly $1/4$ wavelength of the relative wavefunction while in the S=1 state there is a little more than $\lambda/4$ in the well because the potential is slightly stronger. We hypothesize that a similar trick of nature is played also in the case of the $\rho - \rho$ scattering.

We assume that both photons are converted in ρ via vector dominance, and both ρ then interact by a scalar isoscalar potential which is just strong

enough to (almost) bind them for one spin orientation and fails to do so for the other spin orientations. In addition, an isoscalar potential has the desired feature that it cannot exchange charges and does not lead to the $\rho^+\rho^-$ final state.

2. A nonrelativistic potential model

In order to illustrate this idea, we choose a Yukawa-type σ -exchange potential $V(r) = V_0 \exp(-m_\sigma r)/(-m_\sigma r)$. The full process is shown in Fig. 1 and its Lorentz invariant amplitude can be factorized in the following way:

$$M = M_{\gamma\gamma\rho\rho} P_{\rho 1} P_{\rho 2} f_{\rho\pi\pi}^2 . \quad (1)$$

We treat the $\gamma \rightarrow \rho$ conversion and $\rho \rightarrow \pi\pi$ decay perturbatively, but the $\rho\rho \rightarrow \rho\rho$ scattering nonperturbatively by solving the nonrelativistic Schrödinger equation. In the calculation of the matrix element for the process $\gamma_1 \gamma_2 \rightarrow \rho_1 \rho_2$ we account for inelastic scattering of ρ -mesons:

$$M_{\gamma\gamma\rho\rho} = \int \psi_{\gamma\gamma}(\vec{r}_{\gamma 1}, \vec{r}_{\gamma 2}) \hat{V}_{\gamma\rho} \psi_{\rho\rho}(\vec{r}_{\rho 1}, \vec{r}_{\rho 2}) d\vec{r}_{\gamma 1} d\vec{r}_{\gamma 2} d\vec{r}_{\rho 1} d\vec{r}_{\rho 2} \quad (2)$$

where $\hat{V}_{\gamma\rho}$ is the contact $\gamma\rho$ potential $\hat{V}_{\gamma\rho} = (f_{\gamma\rho}^2/M_\rho^3) \delta^3(\vec{r}_{\gamma 1} - \vec{r}_{\rho 1}) \delta^3(\vec{r}_{\gamma 2} - \vec{r}_{\rho 2})$, $\psi_{\gamma\gamma}$ is the function of incident photons (plain wave, normalized in a box of volume V) and $\psi_{\rho\rho}$ is the wave function of the scattered ρ mesons, calculated by solving the Schrödinger equation. The amplitude for $\gamma \rightarrow \rho$ conversion $f_{\gamma\rho}$ is determined from the experimental value for the partial width of the process $\rho \rightarrow e^+e^-$ [8] and is equal to $f_{\gamma\rho}^2/m_\rho^4 = (2.01 * 137)^{-1}$. In eq. (2) the photon selects the correct momentum component (Fourier component) from the calculated scattering wave function of the two mesons.

We account for the shortlived nature of ρ mesons ($\Gamma = 152$ MeV) while writing the propagators of the scattered mesons $P_{\rho 1}$ and $P_{\rho 2}$:

$$P_{\rho i} = \frac{1}{W_{\rho i}^2 - \vec{p}^2 - (m_\rho - \frac{1}{2}i\Gamma)^2} . \quad (3)$$

We reduce the Lorentz invariant four-body phase space $d\Phi_4$ [8] to two-body phase space of the two ρ mesons by integrating over all pion momenta and assuming that the amplitude is not sensitive to them. Neglecting the contributions of order Γ^2/m_ρ^2 we get the cross-section

$$\sigma(W) = \int \frac{(2\pi)^4 |M|^2 d\Phi_4}{2W^2} = \int dm_{\rho 1}^2 \int dm_{\rho 2}^2 \frac{1}{(2\pi)^3} |M_{\gamma\gamma\rho\rho}|^2 \frac{|\vec{p}|}{W^3} \quad (4)$$

$$\times \frac{m_{\rho 1}\Gamma}{(m_{\rho 1}^2 - m_\rho^2)^2 + m_\rho^2\Gamma^2} \frac{m_{\rho 2}\Gamma}{(m_{\rho 2}^2 - m_\rho^2)^2 + m_\rho^2\Gamma^2} ,$$

where $m_{\rho 1}$ and $m_{\rho 2}$ are the effective masses of the scattered ρ -mesons $m_{\rho i}^2 = W_{\rho i}^2 - \vec{p}^2$. This formula (used frequently before) has an intuitive interpretation that the two "final" ρ mesons have arbitrary masses with a Breit-Wigner probability distribution around the nominal mass $m_\rho = 770$ MeV.

Since the scattering phase shift is very sensitive to potential parameters as well as on ρ masses we do calculate it separately for each combination of the two ρ masses and add up the contributions in the double integral numerically, with the appropriate Breit-Wigner weights.

The calculated cross sections $\sigma(W)$ are very sensitive to potential strength V_0 and weakly sensitive to potential range $1/m_\sigma$ (in this nonrelativistic model, $m_\sigma = 550$ MeV is taken). Results for different V_0 are presented in Fig. 2.

For a narrow range of the model parameter V_0 , the results qualitatively agree with the experimental data, as long as we are considering the height of the peak in the $(2^+, 2)$ channel. The position of the peak comes, however, too high above the nominal threshold. Similar calculation using relativistic Klein-Gordon equation for the ρ -meson scattering on fixed potential shows, that the tendency of relativistic effect is to pull the peak down to lower energies. It will be, however, shown in Sect. 3 that a more severe calculation including relativistic effects and gauge invariant coupling can cure this deficiency of the toy model.

In order to get a very low cross section in the $(2^+, 0)$ channel one has to assume a strong spin dependence of the σ -exchange potential. Such strong spin dependence is arbitrary in the present nonrelativistic model, but it will in fact appear in the relativistic model in Sect.3 as a consequence of momentum dependence of the gauge invariant coupling.

3. A relativistic model with gauge invariant $\rho\rho\sigma$ coupling

The Lagrangian, from which we obtain the potential, respects vector dominance and is gauge invariant:

$$\begin{aligned}
\mathcal{L} = & - \frac{1}{4}F_{\mu\nu}(B)F^{\mu\nu}(B) - \frac{1}{4}F_{\mu\nu}(\rho)F^{\mu\nu}(\rho) + \frac{1}{2}m_\rho^2\rho_\mu^2 + \frac{1}{2}(\partial_\mu\sigma)^2 - \frac{1}{2}m_\sigma^2\sigma^2 \\
& + \frac{g_\sigma}{2}\sigma[F_{\mu\nu}(\rho)F^{\mu\nu}(\rho) - \alpha\frac{e}{g}F_{\mu\nu}(\rho)F^{\mu\nu}(B) - \beta(\frac{e}{g})^2F_{\mu\nu}(B)F^{\mu\nu}(B)] \\
& - \frac{1}{2}m_\rho^2[\rho_\mu^2 - (\rho_\mu - \frac{e}{g}B_\mu)^2], \tag{5}
\end{aligned}$$

where $F_{\mu\nu}(\Phi) = \partial_\mu\Phi_\nu - \partial_\nu\Phi_\mu$. After diagonalizing the quadratic term in the Lagrangian, we may want to have a vanishing $\sigma\gamma\gamma$ vertex, as approximately required by the low-energy $\gamma\gamma \rightarrow \pi\pi$ scattering and confirmed in some phenomenological models as the NJL model with a sharp cutoff [9]. This fixes $\beta = 1 - \alpha$. Such an assumption is however not needed in our calculation, since our result in the leading order of e/g does not depend on the parameter β .

The unitary amplitude is calculated with the Bethe-Salpeter equation with the kernel given by Eq. (5). The equation is simplified by the ladder approximation (only σ exchange in the t and u channels) and by taking into account only the leading contributions in powers of e/g . The Blankenbecler-Sugar reduction [10] is used (with no retardation, i.e. with equal off-shellness of the final and intermediate ρ) and the partial wave expansion [11], [12] is performed:

$$\begin{aligned}
M_{\lambda'_1\lambda'_2\lambda_1\lambda_2}^J(q', q) &= V_{\lambda'_1\lambda'_2\lambda_1\lambda_2}^J(q', q) + \int \frac{dk}{k^2 - q_m^2 - i\epsilon} \times \\
& V_{\lambda'_1\lambda'_2\lambda''_1\lambda''_2}^J(q', k) f_{\lambda''_1\lambda''_2}(k) M_{\lambda''_1\lambda''_2\lambda_1\lambda_2}^J(k, q), \tag{6}
\end{aligned}$$

with

$$f_{\lambda''_1\lambda''_2} = \frac{k^2}{(4\pi)^3\sqrt{k^2 + m^2}} a_{\lambda''_1}(\tilde{m}^2(k)) a_{\lambda''_2}(\tilde{m}^2(k)), \tag{7}$$

where $\tilde{m}^2(x) \equiv W^2/4 - x^2$ and the factor

$$a_\lambda(q^2) = \begin{cases} -1 & q^2 < 0 \quad \text{and} \quad \lambda = 0 \\ 0 & q^2 = 0 \quad \text{and} \quad \lambda = 0 \\ +1 & \text{otherwise} \end{cases} \tag{8}$$

takes into account that the longitudinal polarization vector $\epsilon_0^\alpha(q)$ becomes timelike (lightlike) for $q^2 < 0$ ($= 0$).

In eq. (6) the initial particles with polarizations λ_1 and λ_2 have the linear momentum q and are on-shell ($p_1^2 = p_2^2 = W^2/4 - q^2 = 0$). The final (intermediate) ρ mesons with polarizations λ'_1, λ'_2 (λ''_1, λ''_2) can be equally off-shell with $p_3^2 = p_4^2 = W^2/4 - q'^2$ ($W^2/4 - k^2$). If the total energy W is larger than the nominal threshold $2m$, then $q_m^2 \equiv W^2/4 - m^2 > 0$ and eq. (6) has complex solutions as required by unitarity.

Taking special linear combinations of amplitudes with definite polarizations one gets amplitudes with definite parity. Each channel gets decoupled from the others and can be represented by a system of one-dimensional integral equations. The system for the $(2^+, 2)$ channel is explicitly given in Appendix A. These equations were then solved with the matrix inversion method [13], taking 24 points for the magnitude of the relative three-momentum from 0 to the cutoff Λ . It was also checked, that the results change slightly, if one takes only 16 grid points (the differences get however larger with energy, that is why we limited our calculation up to $W = 1.8$ GeV).

The cross section was then calculated by weighing the amplitude squared with two Breit-Wigner factors (one for each final ρ). The approximation of equal off-shellness of the two ρ , with which the Bethe-Salpeter equation (6) was derived and solved, is equivalent to the approximation that the amplitude depends only on the sum of the "masses" of the final ρ . For the total cross-section we get

$$\sigma_{TOT} = \int_0^{\tilde{m}(2m_\pi)} dq' \rho(q') \frac{1}{4} \sum_{J, \lambda_i^{(J)}} (2J+1) |M_{\lambda'_1 \lambda'_2 \lambda_1 \lambda_2}^{(J)}(q', q)|^2, \quad (9)$$

where a first integration is already hidden in

$$\rho(q') = K \left(\frac{q'}{W^2}\right)^2 \int_0^{\tilde{m}(q')-2m_\pi} dp' [\tilde{m}^2(p') + \tilde{m}^2(q') - \tilde{m}^2(0)] \frac{\tilde{m}(p')}{\tilde{m}(q')} \times \\ F_{BW}((\tilde{m}(q') + p')^2, m_\rho^2) F_{BW}((\tilde{m}(q') - p')^2, m_\rho^2), \quad (10)$$

where $K = [(e/g)(1 - \alpha/2)]^4 / (8\pi^5)$. The relativistic Breit-Wigner factor is defined as

$$F_{BW}(p^2, m_\rho^2) = \frac{m_\rho \Gamma_\rho(p^2)}{(p^2 - m_\rho^2)^2 + m_\rho^2 \Gamma_\rho^2(p^2)} \quad (11)$$

with the same p^2 -dependent ρ -meson decay width [14] as in the experimental analysis [2]:

$$\Gamma_\rho(p^2) = \Gamma_\rho(m_\rho^2) \left(\frac{p^2 - 4m_\pi^2}{m_\rho^2 - 4m_\pi^2} \right)^{\frac{3}{2}} \frac{2(m_\rho^2 - 4m_\pi^2)}{(p^2 - 4m_\pi^2) + (m_\rho^2 - 4m_\pi^2)}. \quad (12)$$

with $m_\rho = 770$ MeV, $\Gamma_\rho(m_\rho^2) = 152$ MeV and $m_\pi = 140$ MeV.

The cross sections in separate channels are obviously only part of the total cross section (9). The explicit expression for the $(2^+, 2)$ channel is given in Appendix A.

We take for the vector dominance factor $e/g =$ from $g^2/(4\pi) = 2.3$ [16]. The remaining parameter α were fitted to the experimental data in order to get the correct height of the cross section (the position of the peak and the relative contributions of different channels are however not dependent on α). We have checked that the fitted value for α gives a small enough (10^{-4}) branching ratio for $\rho^0 \rightarrow \gamma\pi^0\pi^0$ decay, which is not observed experimentally. The mass in the two-body propagator after the Blankenbecler-Sugar reduction would be $m = m_\rho = 0.77$ GeV for non-decaying ρ , but can be slightly modified in the more realistic case of broad ρ mesons. We used the value $m = 0.692$ GeV. Since we are interested in the energy range $1.4 \text{ GeV} < W < 1.8 \text{ GeV}$ and since $m < W/2$ the obtained amplitudes are unitary. We checked that the cross sections behave similarly for $W > 2m$, if a different value for m is chosen. It came also out, that the results are relatively insensitive to the choice of the σ mass, so that we will show only the cross sections for $m_\sigma = 0.5$ GeV.

The results for the interesting channels are shown in Fig. 3, for different choices of the free model parameters Λ , g_σ and α together with the experimental values. We checked also that there is a combination of the three free parameters in a reasonable range, which reproduces quite well the experimental results: if we fix one of them, the other two are rather precisely constrained by the data.

4. Conclusion

We have shown that there exist plausible sets of parameters for potential scattering (for the $\rho\rho\sigma$ coupling) such that the peak in the $\rho^0\rho^0$ ($2^+, 2$) channel at $1.4 - 1.8$ GeV is reproduced while in other channels the cross section remains small. The parameters are plausible if compared to the σ -exchange contribution of the N-N interaction (for example in Bonn potential [15]). The agreement does not prove that the mechanism is just potential scattering, but it presents potential scattering as a candidate until proven otherwise. Of course, we neither prove that resonance scattering through a $qq\bar{q}\bar{q}$ molecule is wrong, we only show that it is not conclusive since other mechanisms exist. A finer distinction will be needed.

The success of the potential scattering relies on the choice of model parameters which "hold" about a quarter of the wavelength of the scattered ρ in the "potential well", a situation similar to the singlet $n - p$ scattering where there is also almost exactly a quarter wavelength in the well yielding a high peak at low energy. The nonrelativistic toy model illustrates this point qualitatively; the position of the peak comes, however, too high above the nominal threshold. Relativistic effects and gauge invariant momentum dependent coupling cure this deficiency; they also give a strong spin dependence of the σ -exchange potential needed to keep the cross-section low in other channels.

This work was supported by the Ministry of Science and Technology of Slovenia.

APPENDIX A

In this Appendix we will write down some useful formulas for the calculation of the amplitudes and cross sections. We will concentrate only on one specific channel, namely, the most important $(J^P, J_z) = (2^+, 2)$ channel. Similar equations can be (and were) defined also for the other possible channels.

First one has to project the potential to states with definite total angular momentum. This was done integrating the potentials for $\rho\rho$ scattering obtained from the Lagrangian (5) over the scattering angle [11],[12]:

$$V_{\lambda'_1 \lambda'_2 \lambda_1 \lambda_2}^{(J)}(k', k) = 2\pi \int_{-1}^1 d(\cos\theta) V_{\lambda'_1 \lambda'_2 \lambda_1 \lambda_2}(\vec{k}', \vec{k}). \quad (13)$$

Using these quantities one could solve for each J the Bethe-Salpeter equation (6) for the $4 \times 9 = 36$ unknown functions (of q') $M_{\lambda'_1 \lambda'_2 \lambda_1 \lambda_2}^{(J)}$. However, due to parity and Bose symmetry, not all these functions are independent. In fact, they are related by

$$X_{\lambda'_1 \lambda'_2 \lambda_1 \lambda_2}^{(J)}(q', q) = X_{-\lambda'_1 -\lambda'_2 -\lambda_1 -\lambda_2}^{(J)}(q', q), \quad (14)$$

$$X_{\lambda'_1 \lambda'_2 \lambda_1 \lambda_2}^{(J)}(q', q) = X_{\lambda'_2 \lambda'_1 \lambda_2 \lambda_1}^{(J)}(q', q), \quad (15)$$

($X = M$ or V) so that the matrices $M(q', q)$, $M(k, q)$ in $V(q', q)$ in (6) have only 3 independent elements for $J = 0$ and 12 for $J = 2$, while $V(q', k)$ has 5 independent elements for $J = 0$ and 25 for $J = 2$ (the difference comes from the fact that the matrix elements of $V(q', k)$ can have also longitudinally polarized particles in the ket, while only transversal polarizations are allowed for the other, since $W^2/4 - q^2 = 0$).

All the elements $X_{\lambda'_1 \lambda'_2 \lambda_1 \lambda_2}^{(J)}(q', q)$ do not have good parity. Using the equations (14) and taking special linear combinations we can decouple the original Bethe-Salpeter equation (6), obtaining lower dimensional matrix integral equations, one for each (J^P, J_z) .

For example, we get for $(J^P, J_z) = (2^+, 2)$ the following integral equation:

$$\begin{pmatrix} M_{++++}^{(2)} \\ \bar{M}_{+-+-}^{(2)} \\ \bar{M}_{+0+-}^{(2)} \\ M_{00+-}^{(2)} \end{pmatrix} (q', q) = \begin{pmatrix} V_{++++}^{(2)} \\ \bar{V}_{+-+-}^{(2)} \\ \bar{V}_{+0+-}^{(2)} \\ V_{00+-}^{(2)} \end{pmatrix} (q', q) + \int \frac{dk}{k^2 - q_m^2 - i\epsilon} \times \quad (16)$$

$$\begin{pmatrix} \bar{V}_{++++}^{(2)} & V_{++++}^{(2)} & \bar{V}_{++++}^{(2)} & V_{++++}^{(2)} \\ V_{+-+-}^{(2)} & \bar{V}_{+-+-}^{(2)} & \bar{V}_{+-+-}^{(2)} & V_{+-+-}^{(2)} \\ \bar{V}_{+0+-}^{(2)} & \bar{V}_{+0+-}^{(2)} & \bar{V}_{+0+-}^{(2)} & V_{+0+-}^{(2)} \\ V_{00+-}^{(2)} & V_{00+-}^{(2)} & V_{00+-}^{(2)} & V_{00+-}^{(2)} \end{pmatrix} (q', k) \times$$

$$\begin{pmatrix} 2f^+ & 0 & 0 & 0 \\ 0 & 2f^+ & 0 & 0 \\ 0 & 0 & 4f^- & 0 \\ 0 & 0 & 0 & f^+ \end{pmatrix} (k) \begin{pmatrix} M_{++++}^{(2)} \\ \bar{M}_{+-+-}^{(2)} \\ \bar{M}_{+0+-}^{(2)} \\ M_{00+-}^{(2)} \end{pmatrix} (k, q),$$

where we defined two averages

$$\bar{X}_{\lambda'_1 \lambda'_2 \lambda_1 \lambda_2}^{(J)} = \frac{1}{2} (X_{\lambda'_1 \lambda'_2 \lambda_1 \lambda_2}^{(J)} + X_{-\lambda'_1 -\lambda'_2 \lambda_1 \lambda_2}^{(J)}), \quad (17)$$

$$\bar{\bar{X}}_{\lambda'_1 \lambda'_2 \lambda_1 \lambda_2}^{(J)} = \frac{1}{2} (\bar{X}_{\lambda'_1 \lambda'_2 \lambda_1 \lambda_2}^{(J)} + \bar{X}_{\lambda'_2 \lambda'_1 \lambda_1 \lambda_2}^{(J)}), \quad (18)$$

and where

$$f^\pm(k) = \frac{k^2 a^\pm (W^2/4 - k^2)}{(4\pi)^3 \sqrt{k^2 + m^2}} \quad (19)$$

and $a^+(x) = +1$, $a^-(x) = +1, 0, -1$ for $x = +1, 0, -1$ respectively.

The cross section in this same channel is then

$$\begin{aligned} \frac{1}{\rho(q')} \frac{d\sigma^{(2^+,2)}}{dq'} &= 5(|M_{++++}^{(2)}(q', q)|^2 + |\bar{M}_{+--+}^{(2)}(q', q)|^2 + \\ &2|\bar{M}_{+0+-}^{(2)}(q', q)|^2 + \frac{1}{2}|M_{00+-}^{(2)}(q', q)|^2). \end{aligned} \quad (20)$$

References

- [1] M. Cvetič, B. Golli, N. Mankoč-Borštnik and M. Rosina, Nucl. Phys. **A395** (1983) 349; Y. Fujiwara and K.T. Hecht, Nucl.Phys. **A451** (1986) 625; **A462** (1987) 621.
- [2] ARGUS Coll., H. Albrecht et al., Z. Phys. **C50** (1991) 1.
- [3] ARGUS Coll., H. Albrecht et al., Phys. Lett. **267B** (1991) 535.
- [4] N.N. Achasov, V.A. Karnakov and G.N. Shestakov, Int. J. of Mod. Phys. **A5** (1990) 2705; N.N. Achasov, S.A. Devyanin and G.N. Shestakov, Z. Phys. **C16** (1982) 55, Phys. Lett. **108B** (1982) 134, Z. Phys. **C27** (1985) 99.

- [5] B.A. Li and K.F. Liu, Phys. Lett. **118B** (1982) 435, Phys. Rev. Lett. **51** (1983) 1510, Phys. Rev. **D30** (1984) 613, Phys. Rev. Lett. **58** (1987) 2288.
- [6] B. Moussallam, Z. Phys. **C39** (1988) 535.
- [7] M. Hatzis and J. Paschalis, Lett. al Nuovo Cimento **40** (1984) 362.
- [8] Review of Particle Properties 1994, Phys. Rev. **D 50** (1994) 1173.
- [9] B. Bajc, A.H. Blin, B. Hiller, M.C. Nemes and M. Rosina, Zeit. f. Phys. **A350**, (1994), 229.
- [10] R. Blankenbecler and R. Sugar, Phys. Rev. **142** (1966) 1051.
- [11] M. Jacob and G.C. Wick, Ann. of Phys. **7** (1959) 404.
- [12] F. Gross, J.W. Van Orden and K. Holinde, Phys. Rev. **C45** (1992) 2094.
- [13] G.E. Brown, A.D. Jackson and T.T.S. Kuo, Nucl. Phys. **A133** (1969) 481; M. Haftel and F. Tabakin, Nucl. Phys. **A158** (1970) 1.
- [14] J.D. Jackson, Nuovo Cim. **34** (1964) 1644.
- [15] R. Machleidt, K. Holinde and Ch. Elster, Phys. Reports **149** (1987) 1.
- [16] M. Poppe, Int. J. Mod. Phys. **A1** (1986) 545.

FIGURES

Figure 1: Feynman diagram for the process $\gamma\gamma \rightarrow \rho^0\rho^0 \rightarrow \pi\pi\pi\pi$.

Figure 2: The experimental cross sections for the $(2^+, 2)$ channel [2] (dots) and calculated cross sections for three different potential strengths V_0 : $V_0 = 1400$ MeV gives the highest cross section, while $V_0 = 800$ MeV gives the cross section with the same height as the experimental one.

Figure 3: Cross sections for various channels in the relativistic potential model with scalar exchange in comparison with experimental data.

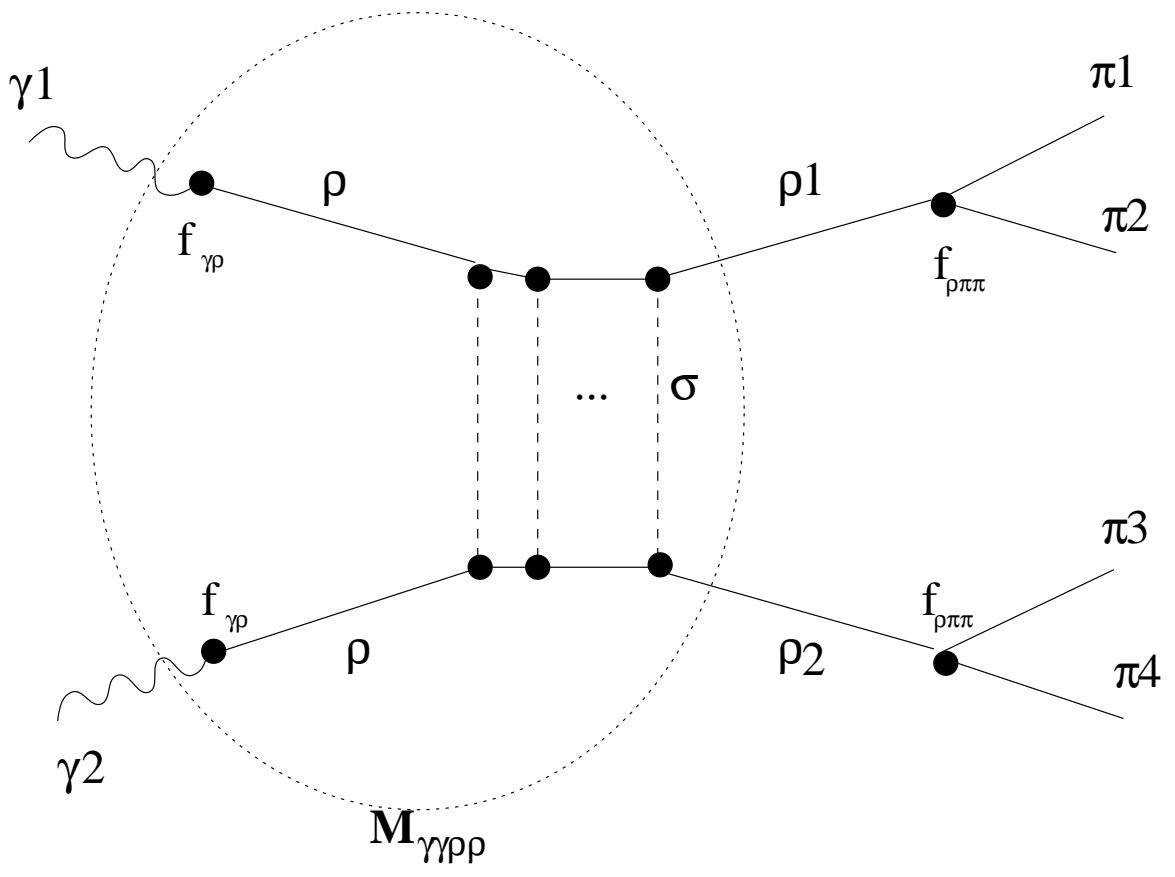
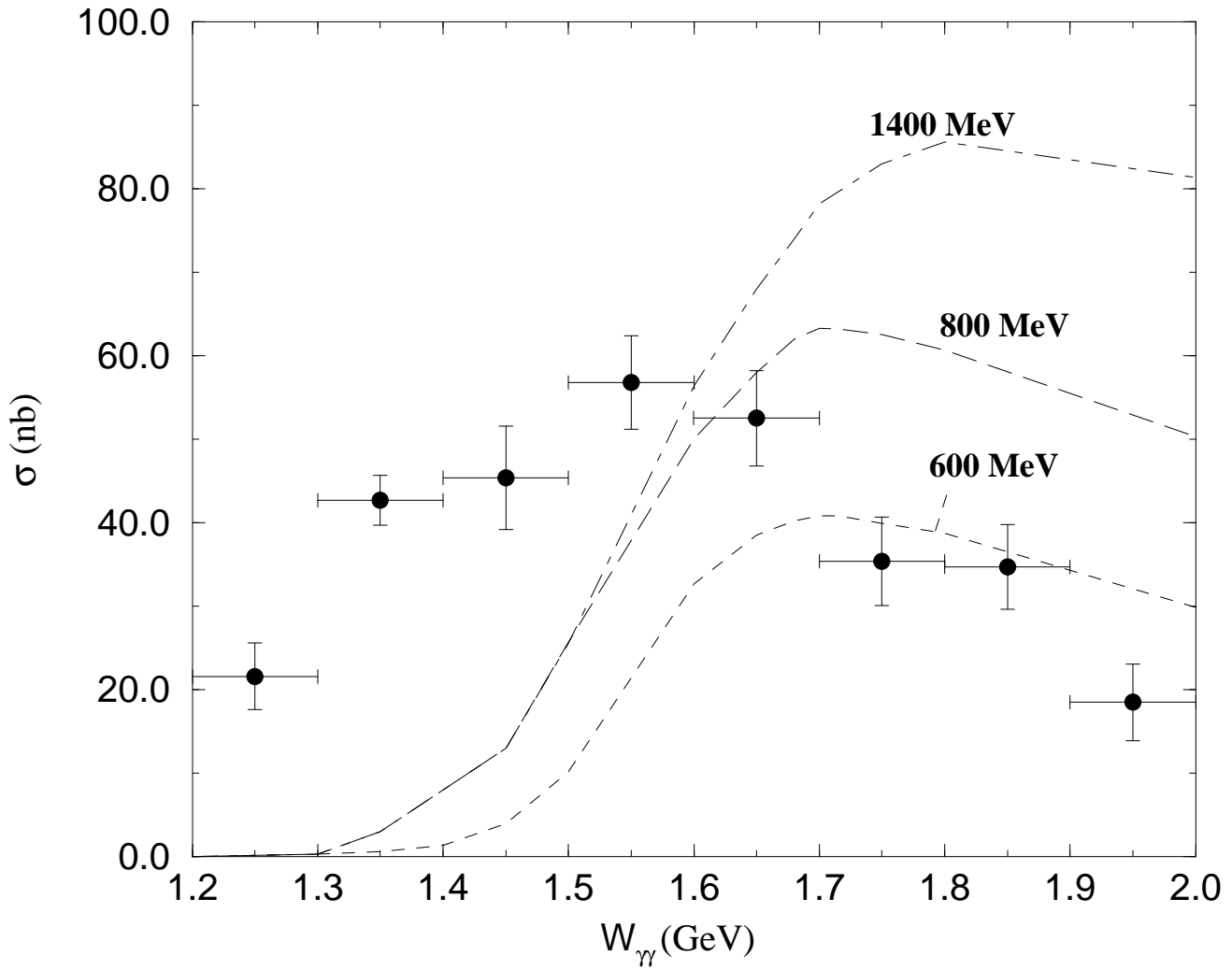


Figure 1

Figure 2

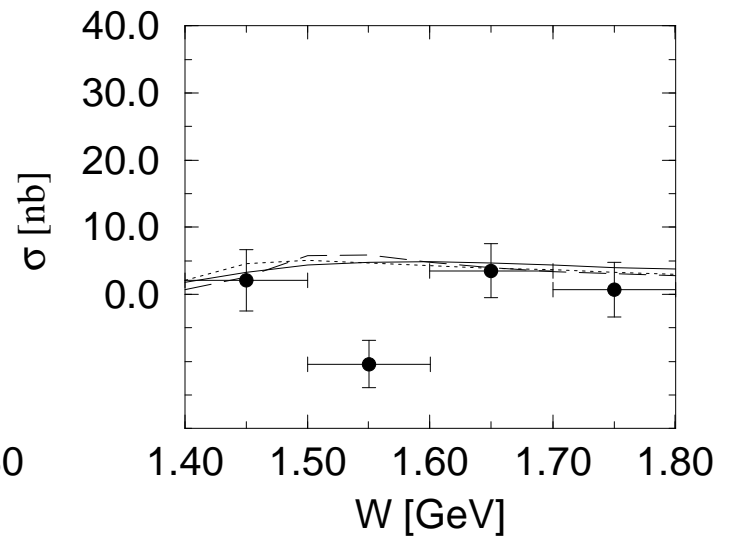
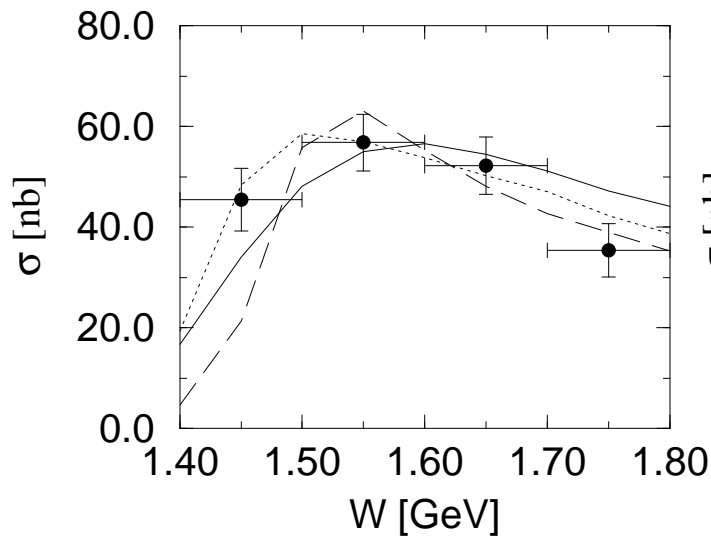


--- $\Lambda=2.4 \text{ GeV}; g_\sigma=9.15 \text{ GeV}^{-1}; \alpha=0.752$
--- $\Lambda=2.6 \text{ GeV}; g_\sigma=8.14 \text{ GeV}^{-1}; \alpha=0.775$

○ ARGUS [3]

$\rho^0 \rho^0 : (2^+, 2)$

$\rho^0 \rho^0 : (2^+, 0)$



$\rho^0 \rho^0 : 0^+$

$\rho^+ \rho^- : \Sigma J^P$

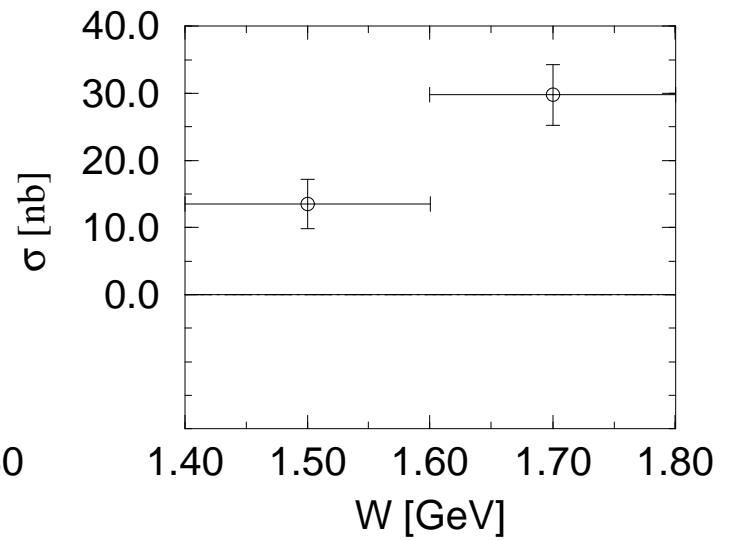
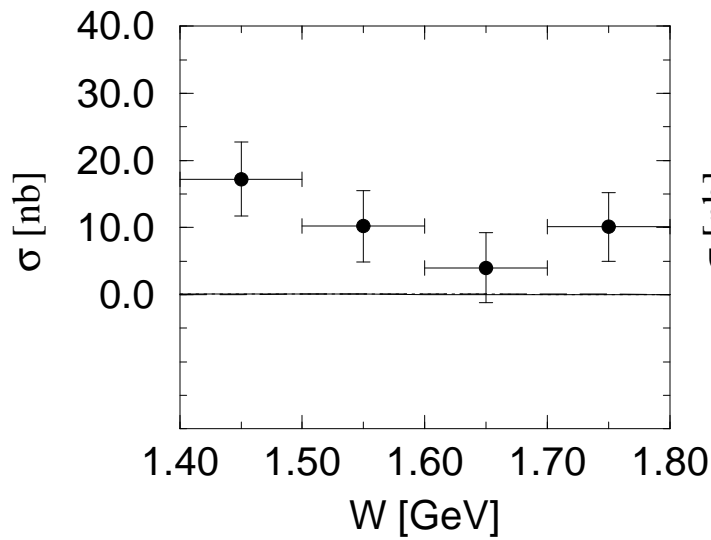


Figure 3